Author Manuscript

Author Manuscript

Author Manuscript

Author Manuscript

HHS Public Access

Author manuscript

Chemistry. Author manuscript; available in PMC 2022 February 16.

Published in final edited form as:

Chemistry. 2020 December 15; 26(70): 16846–16852. doi:10.1002/chem.202003181.

P450 CYP17A1 Variant with a Disordered Proton Shuttle Assembly Retains Peroxo-Mediated Lyase Efficiency

Yilin Liu[a], **Ilia G. Denisov**[b], **Yelena V. Grinkova**[b], **Stephen G. Sligar**[b], **James R. Kincaid**[a]

[a]Departmen of Chemistry, Marquette University 1414W Clybourn Street, Milwaukee, WI 53233 (USA)

[b]Departments of Biochemistry and Chemistry, University of Illinois 116 Morrill Hall, 505 S. Goodwin Avenue, Urbana, IL 61801 (USA)

Abstract

Human cytochrome P450 CYP17A1 first catalyzes hydroxylation at the C17 position of either pregnenolone (PREG) or progesterone (PROG), and a subsequent C_{17}–C_{20} bond scission to produce dehydroepiandrosterone (DHEA) or androstenedione (AD). In the T306A mutant, replacement of the Threonine 306 alcohol functionality, essential for efficient proton delivery in the hydroxylase reaction, has only a small effect on the lyase activity. In this work, resonance Raman spectroscopy is employed to provide crucial structural insight, confirming that this mutant, with its disordered proton shuttle, fails to generate essential hydroxylase pathway intermediates, accounting for the loss in hydroxylase efficiency. Significantly, a corresponding spectroscopic study with the susceptible *lyase* substrate, 17-OH PREG, not only reveals an initially trapped peroxo-iron intermediate experiencing an H-bond interaction of the 17-OH group with the *proximal* oxygen of the Fe-O_p-O_t fragment, facilitating peroxo- attack on the C_{20} carbon, but also unequivocally shows the presence of the subsequent hemiketal intermediate of the lyase reaction.

Introduction

Human cytochrome P450 CYP17A1 plays a critically important role in steroid hormone biosynthesis as an indispensable enzyme involved in the production of androgens.[1, 2] Using pregnenolone (PREG) and progesterone (PROG) as substrates, this human enzyme catalyzes two sequential reactions, namely hydroxylation at the C17 position, and subsequently carbon–carbon bond scission between C17 and C20. The first reaction is typical for P450 chemistry and is driven by classical hydrogen abstraction by a ferryl high-valent intermediate termed Compound I which is followed by “oxygen rebound” that results in the addition of a hydroxyl group to the carbon chain of the substrate.[3] The net result

james.kincaid@mu.edu, s-sligar@illinois.edu.

Supporting information and the ORCID identification number(s) for the author(s) of this article can be found under: https://doi.org/10.1002/chem.202003181.

Experimental Section

Details for expression and purification of CYP17A1 T306A mutant, incorporation into Nanodiscs, preparation of samples for rR Spectroscopy and the resonance Raman measurements can be found in the Supporting Information.

Conflict of interest

The authors declare no conflict of interest.

Author Manuscript Author Manuscript Author Manuscript Author Manuscript

is the “insertion” of an oxygen atom into a C–H bond. Meanwhile, the mechanism of C–C scission reaction, and the nature of catalytically active intermediate involved in this step, are not completely resolved and continue to be a subject of discussion.[4] Compound I driven catalysis utilizing hydrogen abstraction from C17 hydroxyl has been suggested based on experiments using oxygen surrogates[5] and some model compounds[6] although this possibility has been refuted.[7] An alternative mechanism involving the peroxo-iron intermediate via nucleophilic attack on C20, as illustrated in Scheme 1, originally proposed by Akhtar and co-workers,[4, 7, 8] has recently received substantial support in theoretical calculations[9] and experimental studies[10–13] as has been reviewed in detail.[14, 15]

A critical difference between these two mechanisms of P450 catalysis is the obligatory requirement of two sequential protonation events at the distal oxygen atom of iron-coordinated dioxygen moiety, ultimately from solvent water, to form Compound I. The first converts the iron peroxoanion to the hydroperoxo with the second reducing the O–O bond order,[16] breaking this bond, releasing water to form Compound I (CpdI). On the other hand, catalysis by the peroxoanion does not require, and would in fact be inhibited by, proton transfer to the distal oxygen. The efficient proton delivery mechanism for Cpd1 formation is known as an essential feature of productive P450 hydroxylase activity.[17, 18] Specifically, the highly conserved acid-alcohol pair (Asp or Glu followed by Thr or Ser) in the I-helix near the heme iron oxygen and substrate binding site has been shown to be critical for supporting these protonation events. When absent, the substrate can provide the alcohol functionality in some cases[19] or when CpdI is not used as in some prostaglandin biosynthetic steps.[20] The role of the acid/alcohol pair has been revealed by numerous mutational studies. For example, in P450 CYP101 replacing the threonine alcohol side chain with an alanine (T252A) abolished hydroxylation, releasing essentially all the reducing equivalents as hydrogen peroxide.[21] Similar results were observed in other P450 systems. For example, mutations T268A in CYP102A1,[22] T302A in CYP2B4[23] and T303A in CYP2E1,[24] in most cases resulted in a dramatic perturbation of proton delivery mechanism and concomitant enzyme uncoupling. Reactions which can be driven by alternative reactive intermediates, such as the peroxoferric and hydroperoxo-ferric complexes, are usually not inhibited and sometimes even activated in these mutants.[24] Taken together, these results suggest that comparison of the functional properties of other cytochromes P450 where this conserved Thr is mutated to Ala should provide useful mechanistic information about structure of catalytically active iron-oxygen intermediate involved in product turnover.

In the human steroid metabolizing P450 CYP17A1 involved in androgen production,[4, 8, 25] the corresponding acid/alcohol pair is E305 and T306. In order to explore the role of proton transfer in this system, both in the first step of hydroxylation at the C-17 position as well as in the subsequent carbon–carbon lyase reaction, we mutated the threonine at position 306 to alanine.[12] We compared the activity of the T306A mutant and wild-type CYP17A1 self-assembled into Nanodiscs for both pregnenolone (Δ5) (PREG) and progesterone substrates (Δ4) (PROG) substrates in C-17 hydroxylation activity.[12] We also compared the reactivity of 17-OH PREG and 17-OH PROG in the carbon-carbon bond scission (lyase) activity.[12] These results, in agreement with earlier studies,[26] demonstrated that the CpdI driven hydroxylation reaction is drastically diminished in the T306A mutant due to the perturbed proton delivery mechanism, while the C–C scission reaction for both substrates

Author Manuscript Author Manuscript Author Manuscript Author Manuscript

was not dramatically changed. This behavior is similar to other examples of mechanistic observations with this conserved threonine mutations in cytochromes P450[23, 24] and can be considered as an indication of a definitive role played by iron-peroxo intermediate in CYP17A1 catalyzed C–C scission reaction. However, further experiments are needed to reveal the detailed mechanistic origin of this altered activity.

In a series of publications, we described a key difference in the active site of P450 CYP17A1 with the 17-OH substrates bound.[10, 13, 27, 28] Critical is the positioning of the 17-OH group of the corresponding Δ4 and Δ5 substrates that allows hydrogen bonding of the substrate alcohol with the heme bound oxygen or peroxo fragment.[10, 27, 28] Resonance Raman (rR) spectroscopy proved to be a most valuable tool to investigate the active site structure and hydrogen bonding network in CYP17A1 and many other heme proteins,[29–31] with recent studies of cytochromes P450 effectively demonstrating its unique potential for revealing differential interactions of active site H-bond donors, including substrates, with the key Fe-O-O fragment of enzymatic intermediates.[27, 32–35] Thus, in rR studies of WT CYP17A1,[10, 13] it was clearly shown that the 17OH-PROG substrate, with its relatively low lyase efficiency, includes donation of an H-bond to the terminal oxygen (O_t) of the Fe-O_p-O_t fragment, whereas the 17-OH PREG substrate, more efficiently undergoing the C–C bond cleavage reaction, adopts a position with its OH-fragment oriented toward the proximal oxygen (O_p). This impressive level of structural definition provides crucial insight into functional variability, as follows. Generally, H-bonding interactions with the bound peroxo-moiety increase its electron density by polarization of the Fe-O-O fragment, as evidenced by a lowering of the ν(O–O) stretching mode for both lyase substrates with their H-bonding OH-fragments. An H-bonding interaction with the terminal oxygen atom (O_t) of the Fe(O_p–O_t) fragment significantly lowers its nucleophilicity, diminishing lyase reactivity and enhancing the probability for eventual protonation to form the hydroperoxo-intermediate and commitment to Cpd I formation. Conversely, an Fe-O_p-O_t fragment experiencing an H-bonding interaction with the proximal oxygen (O_p), as for the enzyme bound with OH PREG, retains significant nucleophilicity of the terminal (O_t) oxygen, thereby facilitating peroxo-attack on the C_{20} carbonyl of this substrate.[9, 16, 36] Finally, it is important to emphasize that these previously reported spectroscopic results obtained for the WT CYP17 samples provided the first direct evidence for the key hemiketal intermediate (shaded area of Scheme 1) expected for this peroxo-mediated lyase reaction.[10, 13] As will be seen below, corresponding data obtained herein for the T306A variant of CYP17 document the appearance of this same intermediate, confirming the competence of this variant in catalyzing this critical lyase reaction.

Given the significance of a stable membrane bilayer anchor for the protein involved and the need for maintaining well-behaved ligand binding and stabilizing the unstable intermediates,[11, 37] we combined the Nanodisc system with this powerful rR technique to evaluate the role of the T306 residue of the conserved acid/alcohol pair in the active site of human CYP17A1. In this publication, rR spectra of the T306A variant of CYP17A1, in the presence of both the hydroxylase (PREG) and lyase (OH-PREG) substrates, are reported. The results obtained for the unstable dioxy- and peroxo- intermediates demonstrate that the proton shuttle is severely disordered, with no stable ferric-hydroperoxo intermediate observed in the presence of hydroxylation substrate PREG. On the other hand, the carbon–carbon lyase

Author Manuscript Author Manuscript Author Manuscript Author Manuscript

activity is maintained in the mutant, as reported earlier.[12] We have now documented, by rR spectroscopy, the hydrogen bonding interactions involving the 17-hydroxyl group and associated active site water molecules. The ferrous dioxygen adduct is seen to proceed through vibrationally characterized peroxo- and telltale peroxo-hemiketal[10] intermediates, which eventually lead to the DHEA product. Of special interest is the fact that the behavior of the iron-oxygen vibrational frequencies, ν(Fe–O), for the peroxo-intermediates of WT and T306A variant are consistent with the previously reported variations in the lyase efficiencies of the two proteins,[12] suggesting that the efficiency of the lyase reaction is at least partially controlled by the strength and directionality of this H-bonding interaction.

Results and Discussion

As demonstrated in many previously published works, resonance Raman (rR) spectroscopy has been proven to be a powerful method to define the active site structure of Cytochrome P450s, being especially effective for the characterization of the status of the Fe-O-O fragment in unstable enzymatic intermediates.[10, 13, 15, 27, 28, 35, 38–43] Inasmuch as the ν(Fe–O) and ν(O–O) internal modes of the Fe-O-O fragment are often weak, and sometimes obscured by the more strongly enhanced heme modes, plotting the $^{16}O_2/^{18}O_2$ difference spectrum is helpful in revealing these key modes, which provide crucial structural information related to the hydrogen bonding configurations in the active site.

1. Initial oxygenated intermediate trapped at 77 K

As shown in Figure 1 A, the dioxygen adduct of the pregneno-lone (PREG) bound T306A mutant of CYP17A1 exhibits an isotope sensitive ν(^{16}O–^{16}O) mode at 1137 cm−1, with its corresponding ν(^{18}O–^{18}O) mode appearing at 1070 cm^{-1} . Also seen are the ν(Fe–^{16}O) mode observed at 537 cm−1, with its corresponding ν(Fe–^{18}O) mode appearing at ≈ 507cm^{-1} These isotopic shifts are in reasonable agreement with those theoretically predicted.[44]. These data are to be compared with the rR spectra shown in Figure 1B for the Nanodisc embedded p450 CYP17A1 (ND: CYP17) T306A mutant bound with the *lyase* substrate, OH-PREG. The ν(^{16}O–^{16}O) mode appears at 1134 cm–1,with its corresponding ν(^{18}O–^{18}O) stretching mode occurring at 1066 cm^{-1}. The ν(Fe–^{16}O) mode appears at 530 cm^{-1} with the corresponding ν(Fe–^{18}O) mode at 502 cm^{-1}, noting that this internal mode exhibits a frequency ≈ 7 cm^{-1} below that observed for the hydroxylase substrate, PREG.

As mentioned earlier, the behavior observed for these key vibrational modes serves as a sensitive structural probe of this important Fe-*O*-O molecular fragment. The dioxygen adduct of the OH PREG-bound T306A protein, with its H-bonding 17-OH group, exhibits a ν(O–O) mode which is shifted to lower frequency compared to the PROG-bound enzyme, consistent with that seen for H-bonded forms of other oxy-P450 enzymes,[33,41] and carefully designed model compound studies.[45,46] Importantly, even deeper insight is gained from comparison of the observed ν(Fe–O) modes of these oxy-intermediates. Thus, as was shown in earlier experiments,[28] and supported by computational studies,[35,47,48] H-bonding interactions with the terminal oxygen atom (O_t) of the Fe-O_p-O_t fragment leads to shifts to higher frequency compared to non-H-bonded fragments, while H-bonds to the proximal oxygen (O_p) causes shifts to lower frequency. In the present case, the 7 cm^{-1} shift

Author Manuscript Author Manuscript Author Manuscript Author Manuscript

seen for OH-PREG, as compared to the value observed for the PREG sample, confirms the presence of a hydrogen-bonding interaction with the proximal oxygen of the Fe-Op-Ot fragment, as proposed in Scheme 2.[35] Such behavior is similar with that observed for the wild-type CYP17A1 protein,[10,28] where the ν(Fe–O) mode of hydroxylated substrates is 9 cm^{-1} downshifted from that for the non-H-bonding PREG sample.[28].The essential point is that mutation of this highly conserved Thr306 residue, while possibly causing some rearrangements of the active site structure, apparently results in the persistence of an H-bonding interaction of the substrate, or some other active site group, with the proximal oxygen atom of the Fe-Op-Ot fragment, an interaction that can have important functional consequences (vide supra).

2. The peroxo/hydroperoxo states: Irradiated samples of ND:CYP17A1 T306A bound with PREG

Focusing on the rR spectra obtained for the irradiated samples, the $^{16}O_2$—$^{18}O_2$ difference trace of the irradiated oxygenated ND: CYP17A1 T306A mutant containing PREG is shown in Figure 2. A set of oxygen isotope sensitive modes is clearly seen, with a ν(^{16}O–^{16}O) mode occurring at 811 cm^{-1}, and its corresponding ν(^{18}O–^{18}O) at 774 cm^{-1}; a ν(Fe–^{16}O) mode is observed at 552 cm^{-1}, with its ν(Fe–^{18}O) mode at 527 cm^{-1}. Based on the results from many previous rR studies of peroxo- and hydroperoxo- species in various heme proteins,[15,33,39,42] these modes are most reasonably assigned to aferric peroxo-intermediate.

As shown in Figure S1 in the Supporting Information, the rR spectral results demonstrate that annealing of the PREG-bound T306A sample to 165 K reveals no evidence of oxygen isotope sensitive modes, other than those associated with residual dioxygen adduct appearing at 1137 and 1070 cm–1; i.e., the oxyprecursor species that were not cryoreduced in the irradiation chamber and, being relatively stable, persist even at higher temperatures. It is noted that this behavior represents a drastic departure from the wild-type (WT) enzyme, where in earlier studies it was shown that the peroxo- intermediate of the PREG-bound sample of WT ND: CYP17A1 begins to convert to the hydroperoxo-intermediate even at 77 K, converting fully to the protonated species at 165 K.[10] This present result reflects the well-established tendency for the TxxxA mutation of the highly conserved “proton shuttle” assembly of many P450s, including the T252A variant of CYP101,[49–52] to disarrange productive proton transfer and destabilize the iron-hydroperoxo intermediate. While the hydroperoxo-intermediate was observed for the T252A variant of CYP101, our results for T306A CYP17 provide no evidence for its formation at 77 K or at 165 K, though its formation and disappearance at intermediate temperatures cannot be ruled out. However, as was the case for the T252A mutation of CYP101, the T306A replacement in CYP17 presumably causes destabilization of this species, preventing subsequent protonation-assisted O–O bond cleavage and formation of Compound I. In the absence of effective proton delivery, the peroxo-intermediate degrades at higher temperatures, being released eventually as a hydrogen peroxide by-product due to the disordered proton shuttle assembly and highly decoupled hydroxylase chemistry.[18–21, 49–52]

Author Manuscript Author Manuscript Author Manuscript Author Manuscript

3. Irradiated samples of ND:CYP17A1 T306A bound with OH-PREG

Figure 3 A shows the rR spectra of the 17OH-PREG-bound CYP17A1 T306A mutant, where this *lyase* substrate contains an additional H-bonding 17-OH group. The initial product of cryoradiolysis exhibits a clear positive band at 795 cm–1, shifting to lower energy by 37 cm–1 upon $^{18}O_2$ substitution. The corresponding ν(Fe–^{16}O) mode occurs at 547 cm–1 (Δ16/18=25 cm–1). As summarized above for the dioxygen adducts, a large amount of structural information is realized by comparing these results with those obtained for the hydroxylase substrate, PREG, given in Figure 2 and Figure S1. The 16 cm–1 down shift of the ν(O–O) mode, relative to that of the PREG-bound enzyme, documents the presence of an H-bonded ferric peroxo- species, while the ≈5 cm–1 lower frequency of the ν(Fe–O) frequency seen for the OH-PREG-bound T306A peroxo form compared to that of the PREG-bound sample (552 cm–1), suggests the presence of an H-bonding interaction between the -OH group of this lyase substrate and the *proximal* oxygen (O_p) of the Fe-O_p-O_t fragment;[10, 13] i.e., this H-bonding pattern persists in the peroxo species. As discussed above and in several publications,[16, 28, 36] such an H-bonding arrangement retains substantial nucleophilicity of the terminal oxygen atom (O_t) of the peroxo group favoring lyase catalysis.

Given the results obtained for the hydroxylase substrate, PREG, it is not surprising that, even upon annealing the sample containing OH-PREG to 165 K, the rR spectra show no evidence for formation of the hydroperoxo- intermediate (Figure 3 B), where it is seen that only the modes associated with the peroxo-intermediate are retained. However, it is interesting to note that the intensity of the ν(O–O) mode of the peroxo-intermediate (795 cm–1) has decreased relative to the intensity of the 1134 cm–1 mode observed for the residual oxyP450 precursor; i.e., the remaining dioxygen adduct that was not reduced in the irradiation chamber, and is relatively stable even at temperatures above 165 K, provides a reliable internal standard to compare the amount of the peroxo- intermediate before and after annealing. The evident decrease in the amount of the peroxo-intermediate signals a decay of this species and possible conversion to another intermediate that is not enhanced with 442 nm excitation. To this point, it is noted that earlier rR spectroscopic results obtained for the WT protein, using violet excitation lines (406.7 nm), documented the presence of the intermediate depicted in the center of Scheme 1,[10, 13] a species which spontaneously converts to the DHEA lyase product.[10]

Similar experiments were conducted here for the T306A mutant, using the 406.7 nm excitation line of the krypton ion laser. The rR difference spectrum for the same OH-PREG-bound T306A sample that had been annealed to 165 K is shown in such results are in good agreement with the earlier functional studies demonstrating that the T306A mutation of CYP17A1 dramatically diminished the hydroxylase activity, with the product formation rate reduced by 94 %.[12] However, the C–C lyase chemistry conducted by CYP17A1 T306A mutant was not largely impacted, showing a similar rate of NADPH oxidation (21 vs. 17 nmol min–1 nmol–1 P450 for WT and T306A mutant) and a slight different coupling efficiency (4 % vs. 2% for WT and T306A mutant).[12] This important finding reveals that the T306A CYP17A1 variant, for which the proton shuttle is disordered and unable to support Compound I formation, maintains lyase activity via a nucleophilic peroxo-

Author Manuscript Author Manuscript Author Manuscript Author Manuscript

intermediate (Figure 3 B) and remains competent to facilitate the C–C bond cleavage reaction, forming the same key peroxo-hemiketal intermediate (Figure 3 C) depicted in Scheme 1 for the WT enzyme.

4. Structural insight for the mechanism of lyase activity in CYP17.

The rR spectroscopic studies described in this publication using the T306A mutant of human P450 CYP17A1 incorporated into Nanodiscs (ND:CYP17A1 T306A) containing the hydroxylase substrate, PREG, clearly demonstrate that the crippled proton shuttle assembly of this mutant, like TxxxA variants of many P450s,[21, 53] fails to stabilize the iron-hydroperoxo intermediate, which is required for a productive hydroxylase pathway. This accounts for the 94 % loss in hydroxylase efficiency. On the other hand, the present rR studies of this enzyme bound with the lyase substrate, 17-OH PREG, reveal the presence of an initially trapped peroxo-intermediate experiencing an H-bond interaction of the 17-OH group with the *proximal* oxygen of the Fe-Op-Ot fragment, an interaction which facilitates the lyase reaction.[28] It has not escaped our attention that the smaller H-bond induced shift of the ν(Fe-O_p) mode observed for the mutant (≈5 cm–1) is approximately one half of that observed for the WT enzyme (≈ 9 cm–1) (see Table 1), mirroring the coupling efficiency observed for this reaction (about 1:2, respectively).[12] This observation is consistent with the proposal that the efficiency of the lyase reaction is at least partially controlled by the strength and directionality of this H-bonding interaction, critically depending upon substrate positioning with respect to dioxygen moiety.[10, 13]

Conclusion

While the WT CYP17A1 efficiently catalyzes both the hydroxylase and lyase reactions of susceptible substrates, the T306A mutant, with its disordered proton delivery network, exhibits only residual hydroxylase activity, but retains significant lyase efficiency.[12] The resonance Raman spectroscopic studies conducted here confirm that, in the presence of the typical hydroxylase substrate PREG, this variant fails to stabilize the key ferric-hydroperoxo intermediate, thereby accounting for the greatly diminished hydroxylase efficiency. Most significantly, this mutation did not significantly affect lyase activity with the substrate, 17OH-PREG; i.e. , upon annealing to 165 K, the peroxo-ferric complex, documented at 77 K, converts to the hemiketal intermediate, whose characteristic Raman signature was observed with 406.7 nm excitation, a result quite similar to our previous results for the wild-type CYP17A1 protein.[10] This new resonance Raman spectroscopic result provides additional evidence for the *peroxo-mediated* C_{17}–C_{20} scission mechanism of 17OH-PREG in CYP17A1.

Supplementary Material

Refer to Web version on PubMed Central for supplementary material.

Acknowledgements

We acknowledge grant support from the National Institutes of Health, MIRA R35GM118145 (S.G.S.), R01 GM110428 (J.R.K.) and R01 GM125303 (J.R.K.). We appreciate the help provided by Dr. Jay A. LaVerne, Notre

Author Manuscript Author Manuscript Author Manuscript Author Manuscript

Dame Radiation Laboratory (Notre Dame University, IN), a facility of the US Department of Energy, Office of Basic Energy Science.

References

[1]. Nakajin S, Hall PF, J. Biol. Chem 1981, 256, 3871–3876. [PubMed: 6971291]

[2]. Yadav R, Petrunak EM, Estrada DF, Scott EE, Mol Cell Endocrinol 2017, 441, 68–75. [PubMed: 27566228]

[3]. Groves JT in Cytochrome P450 : Structure, Mechanism, and Biochemistry, 3rd ed. (Ed.: Ortiz de Montellano PR), Kluwer Academic/Plenum, New York, 2005, pp. 1–43.

[4]. Akhtar M, Write JN in Monooxygenase, Peroxidase and Peroxygenase Properties and Mechanisms of Cytochrome P450 (Eds.: Hrycay EG, Bandiera SM), Springer International, Switzerland, 2015, pp. 107–130.

[5]. Yoshimoto FK, Gonzalez E, Auchus RJ, Guengerich FP, J. Biol. Chem 2016, 291, 17143–17164. [PubMed: 27339894]

[6]. Gonzalez E, Johnson KM, Pallan PS, Phan TTN, Zhang W, Lei L, Wawrzak Z, Yoshimoto FK, Egli M, Guengerich FP, J. Biol. Chem 2018, 293, 541–556. [PubMed: 29212707]

[7]. Akhtar M, Corina D, Miller S, Shyadehi AZ, Wright JN, Biochemistry 1994, 33, 4410–4418. [PubMed: 8155659]

[8]. Akhtar M, Wright JN, Lee-Robichaud P, J. Steroid Biochem. Mol. Biol 2011, 125, 2–12. [PubMed: 21094255]

[9]. Bonomo S, Jorgensen FS, Olsen L, J. Chem. Inf. Model 2017, 57, 1123–1133. [PubMed: 28387522]

[10]. Mak PJ, Gregory MC, Denisov IG, Sligar SG, Kincaid JR, Proc. Natl. Acad. Sci. USA 2015, 112, 15856–15861. [PubMed: 26668369]

[11]. Gregory MC, Denisov IG, Grinkova YV, Khatri Y, Sligar SG, J. Am. Chem. Soc 2013, 135, 16245–16247. [PubMed: 24160919]

[12]. Khatri Y, Gregory MC, Grinkova YV, Denisov IG, Sligar SG, Biochem. Biophys. Res. Commun 2014, 443, 179–184. [PubMed: 24299954]

[13]. Mak PJ, Duggal R, Denisov IG, Gregory MC, Sligar SG, Kincaid JR, J. Am. Chem. Soc 2018, 140, 7324–7331. [PubMed: 29758981]

[14]. Ortiz de Montellano PR in Cytochrome P450 : Structure, Mechanism, and Biochemistry, 4th ed. (Ed.: Ortiz de Montellano PR), Springer International Publishing, New York, 2015, pp. 111–176.

[15]. Mak PJ, Denisov IG, Biochim. Biophys. Acta, Proteins Proteomics 2018, 1866, 178–204. [PubMed: 28668640]

[16]. Harris DL, Loew GH, J. Am. Chem. Soc 1998, 120, 8941–8948.

[17]. Denisov IG, Sligar SG in Cytochrome P450 : Structure, Mechanism and Biochemistry, 4th *ed.* (Ed.: Ortiz de Montellano PR), Springer, Heidel-berg. 2015, pp. 69–109.

[18]. Denisov IG, Makris TM, Sligar SG, Schlichting I, Chem. Rev 2005, 105, 2253–2277. [PubMed: 15941214]

[19]. Nagano S, Cupp-Vickery JR, Poulos TL, J. Biol. Chem 2005, 280, 22102–22107. [PubMed: 15824115]

[20]. Guengerich FP, Munro AW, J. Biol. Chem 2013, 288, 17065–17073. [PubMed: 23632016]

[21]. Martinis SA, Atkins WM, Stayton PS, Sligar SG, J. Am. Chem. Soc 1989, 111, 9252–9253.

[22]. Clark JP, Miles CS, Mowat CG, Walkinshaw MD, Reid GA, Daff SN, Chapman SK, J. Inorg. Biochem 2006, 100, 1075–1090. [PubMed: 16403573]

[23]. Vaz ADN, Pernecky SJ, Raner GM, Coon MJ, Proc. Natl. Acad. Sci. USA 1996, 93, 4644–4648. [PubMed: 8643457]

[24]. Coon MJ, Vaz AD, McGinnity DF, Peng HM, Drug Metab. Dispos 1998, 26, 1190–1193. [PubMed: 9860926]

[25]. Gilep AA, Sushko TA, Usanov SA, Biochim. Biophys. Acta Proteins Proteomics 2011, 1814, 200–209.

[26]. Lee-Robichaud P, Akhtar ME, Akhtar M, Biochem. J 1998, 330, 967–974. [PubMed: 9480917]

Author Manuscript Author Manuscript Author Manuscript Author Manuscript

[27]. Gregory MC, Mak PJ, Khatri Y, Kincaid JR, Sligar SG, Biochemistry 2018, 57, 764–771. [PubMed: 29283561]

[28]. Gregory M, Mak PJ, Sligar SG, Kincaid JR, Angew. Chem. Int. Ed 2013, 52, 5342–5345; Angew. Chem. 2013, 125, 5450–5453.

[29]. Mak PJ in Handbook of Porphyrin Science (Eds.: Kadish KM, Smith K, Guilard R), World Scientific Publishing, Singapore, 2016, 42, 1–120.

[30]. Milazzo L, Tognaccini L, Howes BD, Smulevich G, J. Raman Spectrosc 2018, 49, 1041–1055.

[31]. El-Mashtoly SF, Kitagawa T, Pure Appl. Chem 2008, 80, 2667–2678.

[32]. Zhu QH, Mak PJ, Tuckey RC, Kincaid JR, Biochemistry 2017, 56, 5786–5797. [PubMed: 28991453]

[33]. Denisov IG, Mak PJ, Makris TM, Sligar SG, Kincaid JR, J. Phys. Chem. A 2008, 112, 13172–13179. [PubMed: 18630867]

[34]. Mak PJ, Denisov LG, Victoria D, Makris TM, Deng TJ, Sligar SG, Kincaid JR, J. Am. Chem. Soc 2007, 129, 6382–6383. [PubMed: 17461587]

[35]. Soldatova VA, Spiro TG, J. Inorg. Biochem 2020, 207, 111054–111062. [PubMed: 32217351]

[36]. Ogliaro F, de Visser SP, Cohen S, Sharma PK, Shaik S, J. Am. Chem. Soc 2002, 124, 2806–2817. [PubMed: 11890833]

[37]. Duggal R, Liu YL, Gregory MC, Denisov IG, Kincaid JR, Sligar SG, Biochem. Biophys. Res. Commun 2016, 477, 202–208. [PubMed: 27297105]

[38]. Mak PJ, Thammawichai W, Wiedenhoeft D, Kincaid JR, J. Am. Chem. Soc 2015, 137, 349–361. [PubMed: 25506715]

[39]. Mak PJ, Luthra A, Sligar SG, Kincaid JR, J. Am. Chem. Soc 2014, 136, 4825–4828. [PubMed: 24645879]

[40]. Aono S, Kato T, Matsuki M, Nakajima H, Ohta T, Uchida T, Kitagawa T, J. Biol. Chem 2002, 277, 13528–13538. [PubMed: 11821422]

[41]. Tosha T, Kagawa N, Arase M, Waterman MR, Kitagawa TT, J. Biol. Chem 2008, 283, 3708–3717. [PubMed: 18032381]

[42]. Ohta T, Liu JG, Naruta Y, Coord. Chem. Rev 2013, 257, 407–413.

[43]. Sjodin T, Christian JF, Macdonald IDG, Davydov R, Unno M, Sligar SC, Hoffman BM, Champion PM, Biochemistry 2001, 40, 6852–6859. [PubMed: 11389599]

[44]. Nakamoto K, Infrared and Raman Spectra of Inorganic and Coordination Compounds, Part A: Theory and Applications in Inorganic Chemistry, 6th *ed.*, Wiley, Hoboken, 2009.

[45]. Tani F, Matsu-ura M, Nakayama S, Ichimura M, Nakamura N, Naruta Y, J. Am. Chem. Soc 2001, 123, 1133–1142. [PubMed: 11456666]

[46]. Matsu-ura M, Tani F, Nakayama S, Nakamura N, Naruta Y, Angew.Chem Int Ed 2000, 39, 1989–1991; Angew. Chem. 2000, 112, 2083–2086

[47]. Spiro TG, Soldatova AV, Balakrishnan G, Coord. Chem. Rev 2013, 257,511–527. [PubMed: 23471138]

[48]. Spiro TG, Soldatova AV, J. Inorg. Biochem 2012,115, 204–210. [PubMed: 22824153]

[49]. Nagano S, Poulos TL, J. Biol. Chem 2005, 280, 31659–31663. [PubMed: 15994329]

[50]. Davydov R, Makris TM, Kofman V, Werst DE, Sligar SG, Hoffman BM, J. Am. Chem. Soc 2001, 123, 1403–1415. [PubMed: 11456714]

[51]. Davydov R, Perera R, Jin SX, Yang TC, Bryson TA, Sono M, Dawson JH, Hoffman BM, J. Am. Chem. Soc 2005, 127, 1403–1413. [PubMed: 15686372]

[52]. Kim SH, Yang TC, Perera R, Jin SX, Bryson TA, Sono M, Davy-dov R, Dawson JH, Hoffman BM, Dalton Trans 2005, 3464–3469. [PubMed: 16234926]

[53]. Gerber NC, Sligar SG, J. Am. Chem. Soc 1992, 114, 8742–8743.

Author Manuscript Author Manuscript Author Manuscript Author Manuscript

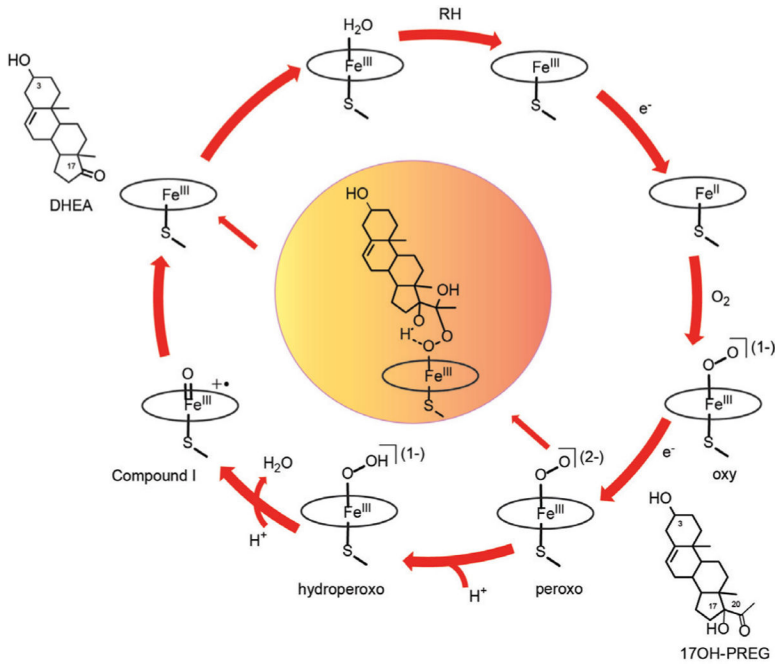

Scheme 1.

Cytochrome P450 17A1 enzymatic cycle and the pathway of formation of peroxo hemiketal following peroxo attack on C20 of the substrate (17OH-PREG).

Author Manuscript Author Manuscript Author Manuscript Author Manuscript

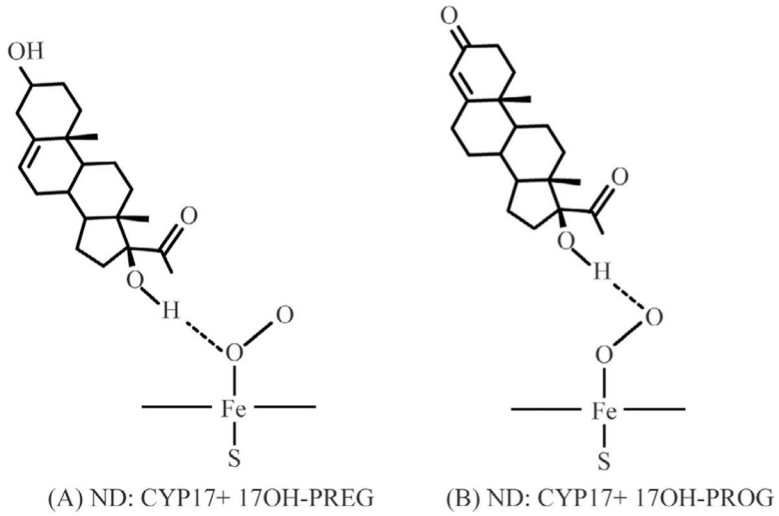

(A) ND: CYP17+ 17OH-PREG (B) ND: CYP17+ 17OH-PROG

Scheme 2.

Cytochrome P450 17A1 protein-substrates H-bond interactions.

Author Manuscript Author Manuscript Author Manuscript Author Manuscript

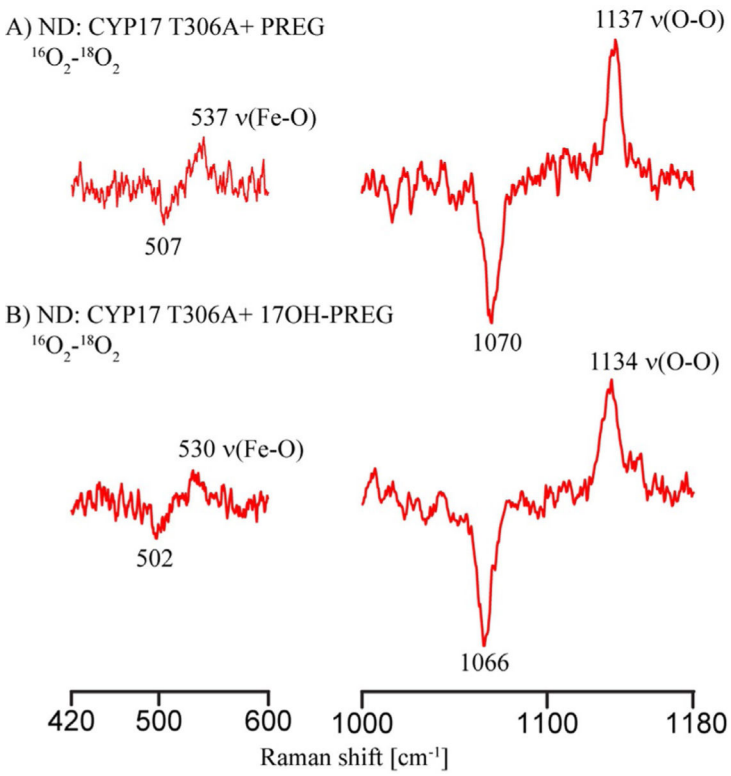

Figure 1.

The rR spectra of $^{16}O_2$–$^{18}O_2$ difference plots of ND: CYP17A1 T306A samples with PREG (A) and 17OH-PREG (B). Spectra were measured using the 413.1 nm excitation line.

Author Manuscript Author Manuscript Author Manuscript Author Manuscript

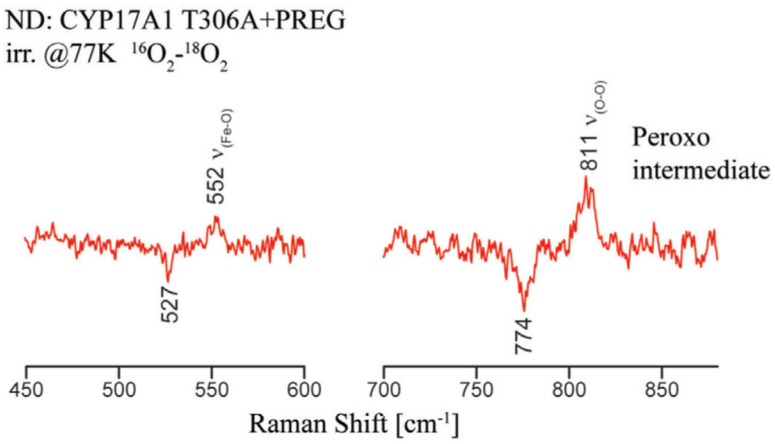

Figure 2.

rR spectra data for irradiated dioxygen adducts of PREG bound CYP 17A1(T306A). Spectra were measured with 442 nm excitation at 77 K.

Author Manuscript Author Manuscript Author Manuscript Author Manuscript

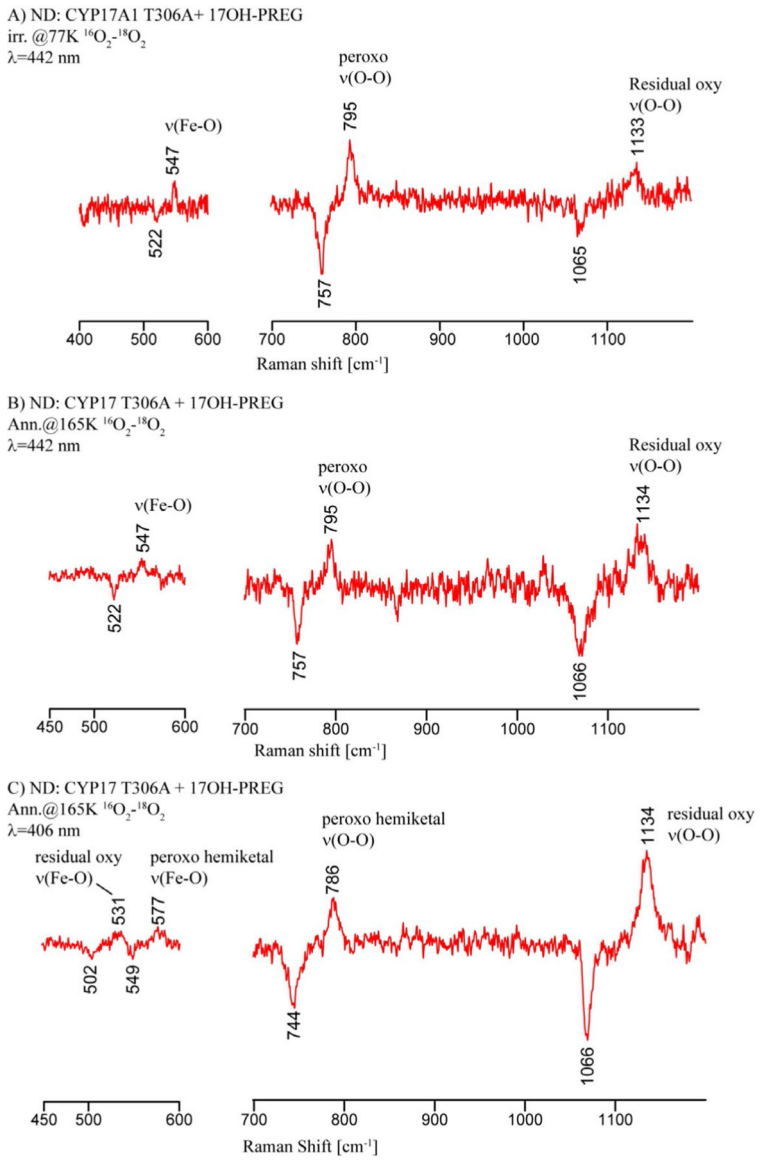

Figure 3.

rR difference spectra data for irradiated and annealed dioxygen adducts of 17OH-PREG bound CYP 17A1(T306A). (A) The rR difference spectrum of irradiated oxy samples. (B) The corresponding samples after annealing to 165 K and spectra were measured with 442 nm excitation line. (C) The corresponding samples after annealing to 165 K and spectra were measured with 406.7 nm excitation line.

Author Manuscript Author Manuscript Author Manuscript Author Manuscript

Table 1.

Summary of the ν(Fe–O) and ν(O–O) Modes in different intermediates for Wild-Type and T306A CYP17A1

	Oxy complex		Peroxo-intermediate		Hydroperoxo-intermediate		Hemiketal-intermediate	
	ν(Fe–O)	**ν (O–O)**	**ν(Fe–O)**	**ν (O–O)**	**ν(Fe–O)**	**ν (O–O)**	**ν(Fe–O)**	**ν (O–O)**
WT PREG	535	1140	554	802	572	775	NA	NA
WT PROG	536	1140	NA	NA	575	772	NA	NA
WT 17OH-PREG	526	1135	546	796	NA	NA	579	791
WT 17OH-PROG	542	1131	562	790	576	771	573	785
T306A PREG	537	1137	552	811	NA	NA	NA	NA
T306A 17OH-PREG	530	1134	547	795	NA	NA	577	786

Chemistry. Author manuscript; available in PMC 2022 February 16.